

Measurement of the radial distribution of Cherenkov light generated by TeV γ -ray air showers

F.A. Aharonian^a, A.G. Akhperjanian^b, J.A. Barrio^{c,d},
 K. Bernlöhner^{a,h}, J.J.G. Beteta^d, H. Bojahr^f, J.L. Contreras^d,
 J. Cortina^d, A. Daum^a, T. Deckers^e, J. Fernandez^{c,d},
 V. Fonseca^d, A. Fraß^a, J.C. Gonzalez^d, G. Heinzelmänn^g,
 M. Hemberger^a, G. Hermann^a, M. Heß^a, A. Heusler^a,
 W. Hofmann^a, H. Hohl^f, I. Holl^b, D. Horns^g, R. Kankanyan^{a,b},
 M. Kestel^c, O. Kirstein^e, C. Köhler^a, A. Konopelko^a,
 H. Kornmayer^c, D. Kranich^c, H. Krawczynski^a, H. Lampeitl^a,
 A. Lindner^g, E. Lorenz^c, N. Magnussen^f, H. Meyer^f,
 R. Mirzoyan^{c,d,b}, A. Moralejo^d, L. Padilla^d, M. Panter^a,
 D. Petry^{c,f}, R. Plaga^c, J. Prahl^g, C. Prosch^c, G. Pühlhofer^a,
 G. Rauterberg^e, W. Rhode^f, A. Röhring^g, M. Samorski^e,
 J.A. Sanchez^d, D. Schmele^g, F. Schröder^f, W. Stamm^e,
 M. Ulrich^a, H.J. Völk^a, B. Wiebel-Sooth^f, C.A. Wiedner^a,
 M. Willmer^e, H. Wirth^a

HEGRA Collaboration

^a*Max-Planck-Institut für Kernphysik, P.O. Box 103980, D-69029 Heidelberg, Germany*

^b*Yerevan Physics Institute, Yerevan, Armenia*

^c*Max-Planck-Institut für Physik, Föhringer Ring 6, D-80805 München, Germany*

^d*Facultad de Ciencias Fisicas, Universidad Complutense, E-28040 Madrid, Spain*

^e*Universität Kiel, Inst. für Kernphysik, Olshausenstr.40, D-24118 Kiel, Germany*

^f*BUGH Wuppertal, Fachbereich Physik, Gaußstr.20, D-42119 Wuppertal, Germany*

^g*Universität Hamburg, II. Inst. für Experimentalphysik, Luruper Chaussee 149, D-22761 Hamburg, Germany*

^h*Now at Forschungszentrum Karlsruhe, P.O. Box 3640, 76021 Karlsruhe*

ⁱ*Now at Department of Physics University of Leeds, Leeds LJ2 9JT, UK*

Abstract

Using air showers induced by TeV γ -rays from Mrk 501, the radial distribution of Cherenkov light is investigated. The shower geometry is reconstructed from the stereoscopic shower images obtained with the telescopes of the HEGRA IACT system. With the core position known to better than 10 m, the light yield as a function of the distance to the shower axis is derived by comparing event-by-event the image intensities measured in the different telescopes. We observe a change in the shape of the light pool with shower energy, and with zenith angle. Data are well reproduced by Monte-Carlo air shower simulations.

1 Introduction

Over the last decade, imaging atmospheric Cherenkov telescopes (IACTs) have emerged as the prime instrument for the detection of cosmic γ -rays in the TeV energy regime [1]. Both galactic and extragalactic sources of such γ -rays have been firmly established, and have been identified with pulsars, supernova remnants, and active galactic nuclei. Going beyond the existence proof for different classes of γ -ray sources, interests are increasingly turning towards precise measurements of the flux and of the energy spectra, and the search for a break or cutoff in the spectra.

Precise measurements of flux and spectrum with the IACT technique represent a non-trivial challenge. Unlike particle detectors used in high-energy-physics experiments or flown on balloons or satellites, Cherenkov telescopes cannot be calibrated in a test beam. Their energy calibration and response function has to be derived indirectly, usually relying heavily on Monte Carlo simulations. In addition, conventional single IACTs do not allow to unambiguously reconstruct the full geometry of an air shower, i.e., its direction in space and its core location; this lack of constraints make consistency checks between data and simulation more difficult.

The stereoscopic observation of air showers with multiple telescopes, as pioneered in the HEGRA system of Cherenkov telescopes [2], solves the latter problem. With two telescopes, the shower geometry is fully determined. With three or more telescopes, the geometry is overdetermined and one can measure resolution functions etc. [3]. Angular resolution and energy resolution is improved compared to a single telescope. The stereoscopic reconstruction of air showers also allows a more detailed study of shower properties.

The analysis presented in the following concentrates on one feature of γ -ray induced air showers which is central to the reconstruction of shower energies,

namely the distribution of photon intensity in the Cherenkov light pool, as a function of the distance to the shower core. In principle, the distribution of Cherenkov light can be calculated from first principles, starting from the shower evolution governed by Quantum Electro Dynamics (QED), followed by the well-understood emission of Cherenkov light, and its propagation through the atmosphere. The relevant atmospheric parameters are quite well known and parameterized (see, e.g., [4,5]). Nevertheless, early simulations showed significant differences between simulation codes [6]. These discrepancies can be traced to differences in the assumptions and in the simplifications which are unavoidable to limit the processor time required to generate a representative sample of air showers. More recently, simulation codes seem to have converged (see, e.g., [7]), and agree reasonably well among each other. Nevertheless, the experimental verification of this key input to the interpretation of IACT data seems desirable. In the past, experimental results concerning the distribution of Cherenkov light in air showers were mainly limited to hadron-induced showers of much higher energies.

The study of the distribution of Cherenkov light in TeV γ -ray showers was carried out using the HEGRA system of IACTs, based on the extensive sample of γ -rays detected from the AGN Mrk 501 [8]. The Mrk 501 γ -ray sample combines high statistics with a very favorable ratio of signal to cosmic-ray background. The basic idea is quite simple: the shower direction and core location is reconstructed based on the different views of the shower. One then selects showers of a given energy and plots the light yield observed in the telescopes as a function of the distance to the shower core. For this event selection, one should not use the standard procedures for energy reconstruction [8,3], since these procedures already assume a certain distribution of the light yield. Instead, a much simpler – and bias-free – method is used to select events of a given energy: one uses a sample of events which have their core at a fixed distance d_i (typically around 100 m) from a given telescope i , and which generate a fixed amount of light a_i in this telescope. Located on a circle around telescope i , these showers cover a wide range in core distance r_j relative to some second telescope j , which in case of the HEGRA array is located between about 70 m and 140 m from telescope i . The measurement of the light yield a_j in this second telescope provides with $a_j(r_j)$ the shape of the Cherenkov light pool. Lacking an absolute energy scale, this method does provide the radial dependence, but not the absolute normalization of the light yield. To determine the distribution of light for pure γ -rays, the cosmic-ray background under the Mrk 501 signal is subtracted on a statistical basis.

The following sections briefly describe the HEGRA IACT system, give more detail on the Mrk 501 data set and the analysis technique, and present and summarize the results.

2 The HEGRA IACT system

The HEGRA IACT system is located on the Canary Island of La Palma, at the Observatorio del Roque de los Muchachos of the Instituto Astrofisico de Canarias, at a height of about 2200 m asl. The system will ultimately comprise five identical telescopes, four of which are arranged in the corners of a square with roughly 100 m side length; the fifth telescope is located in the center of the square. Currently, four of the telescopes are operational in their final form. The fifth telescope – one of the corner telescopes – is equipped with an older camera and will be upgraded in the near future; it is not included in the CT system trigger, and is not used in this analysis.

The system telescopes have 8.5 m^2 mirror area, 5 m focal length, and 271-pixel cameras with a pixel size of 0.25° and a field of view of 4.3° . The cameras are read out by 8-bit Flash-ADCs, which sample the pixel signals at a frequency of 120 MHz. More information on the HEGRA cameras is given in [9]. The two-level trigger requires a coincidence of two neighboring pixels to trigger a telescope, and a coincidence of at least two telescope triggers to initiate the readout. The pixel trigger thresholds were initially set to 10 mV, corresponding to about 8 photoelectrons, and were later in the 1997 run reduced to 8 mV, resulting in a typical trigger rate of 15 Hz, and an energy threshold of the system of about 500 GeV. An in-depth discussion of the trigger system can be found in [10].

During data taking, a light pulser is used to regularly monitor the gain and timing of the PMTs. FADC pedestals and offsets of the trigger discriminators are followed continuously. Deviations in telescope pointing are measured and corrected using bright stars, resulting in a pointing accuracy of better than 0.01° [11].

In the data analysis, a deconvolution procedure is applied to the FADC data to generate minimum-length signals, and a signal amplitude and timing is derived for each pixel [12]. With the gain set to about 1 FADC count per photoelectron, the system provides a direct linear range of about 200 photoelectrons. For larger signals, the pulse length as measured by the FADC can be used to recover the amplitude information, extending the dynamic range to well beyond 500 photoelectrons per pixel. Image pixels are then selected as those pixels having a signal above a high cut of 6 photoelectrons, or above cut of 3 photoelectrons if adjacent to a high pixel. By diagonalizing its ‘tensor of inertia’, the major and minor axes of the images are determined, and the usual *width* and *length* parameters [13]. Both the image of the source of a γ -ray and the point where the shower axis intersects the telescope plane fall onto the major axes of the images. From the multiple views of an air shower provided by the different telescopes, the shower direction is hence determined by super-

imposing the images and intersecting their major axes (see [2,14] for details); the typical angular resolution is 0.1° . Similarly, the core location is derived. The γ -ray sample is enhanced by cuts on the *mean scaled width* which is calculated by scaling the measured *widths* of all images to the *width* expected for γ -ray images of a given image *size* and distance to the shower core [8].

To simulate the properties and detection characteristics of the HEGRA IACT system, detailed Monte-Carlo simulations are available, using either the ALTAI [18] or the CORSIKA [19] air shower generator, followed by a detailed simulation of the Cherenkov emission and propagation and of the detector. These simulations include details such as the pulse shapes of the input signals to the pixel trigger discriminators, or the signal recording using the Flash-ADC system [20,21]. In the following, primarily the ALTAI generator and the detector simulation [20] was used. Samples of simulated showers were available for zenith angles of 0° , 20° , 30° , and 45° . Distributions at intermediate angles were obtained by suitably scaling and/or interpolating the distributions.

3 The Mrk501 data set

The extragalactic VHE γ -ray source Mrk 501 [15,16] showed in 1997 significant activity, with peak flux levels reaching up to 10 times the flux of the Crab nebula (see [17] for a summary of experimental results, first HEGRA results are given in [8]). The telescopes of the HEGRA IACT system were directed towards Mrk 501 for about 140 h, accumulating a total of about 30000 γ -ray events at zenith angles between 10° and 45° . Mrk 501 was typically positioned 0.5° off the optical axis of the telescope, with the sign of the displacement varying every 20 min. In this mode, cosmic-ray background can be determined by counting events reconstructed in an equivalent region displaced from the optical axis by the same amount, but opposite in direction to the source region; dedicated off-source runs are no longer required, effectively doubling the net on-source time. Given the angular resolution of about 0.1° , the separation by 1° of the on-source and off-source regions is fully sufficient. The relatively large field of view of the cameras ensures, on the other hand, that images are reliably reconstructed even with a source displaced from the center of the camera.

The Mrk 501 γ -ray data [8] have provided the basis for a number of systematic studies of the properties of the HEGRA telescopes, and of the characteristics of γ -ray induced air showers (see, e.g., [3]).

For the following analysis, the data set was cleaned by rejecting runs with poor or questionable weather conditions, with hardware problems, or with significant deviations of the trigger rates from typical values. A subset of

events was selected where at least three telescopes had triggered, and had provided useful images for the reconstruction of the shower geometry. Fig. 1 shows the distribution of reconstructed shower axes in the angle θ relative to the direction towards Mrk 501. A cut $\theta^2 < 0.05(^{\circ})^2$ was applied to enhance the γ -ray content of the sample. To further reduce the cosmic-ray background,

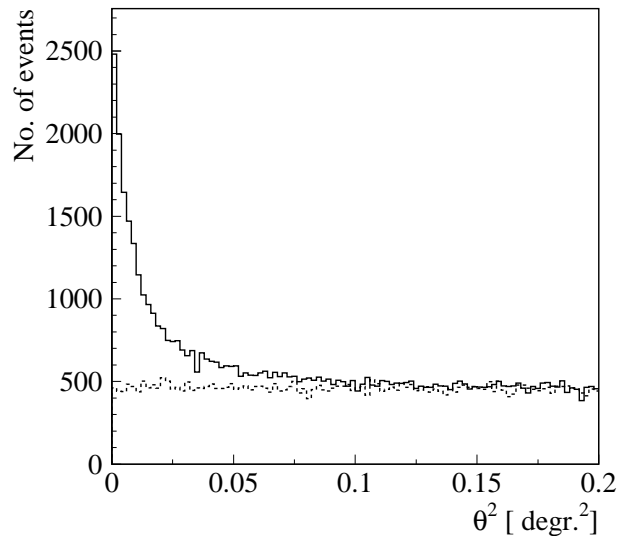


Fig. 1. Distribution in the square of the angle θ between the reconstructed shower axis and the direction to the source, for events with at least three triggered telescopes. No cuts on image shapes are applied. The dashed line shows the distribution for the background region.

a loose cut on the *mean scaled width* was used. The distributions in the *mean scaled width* are shown in Fig. 2; events were selected requiring a value below 1.25; this cut accepts virtually all γ -rays. To ensure that the core location of the events is well reconstructed, the sample was further restricted to events with a core location within 200 m from the center of the array (Fig. 3); in addition, events with $y_{core} > 100$ m were rejected, corresponding to the area near the fifth telescope currently not included in the system. After these cuts, a sample of 11874 on-source events remained, including a background of 1543 cosmic-ray events, as estimated using the equal-sized off-source region.

For such a sample of events at TeV energies, the core location is measured with a precision of about 6 m to 7 m for events with cores within a distance up to 100 m from the central telescope; for larger distances, the resolution degrades gradually, due to the smaller angles between the different views, and the reduced image *size* (see Fig. 4).

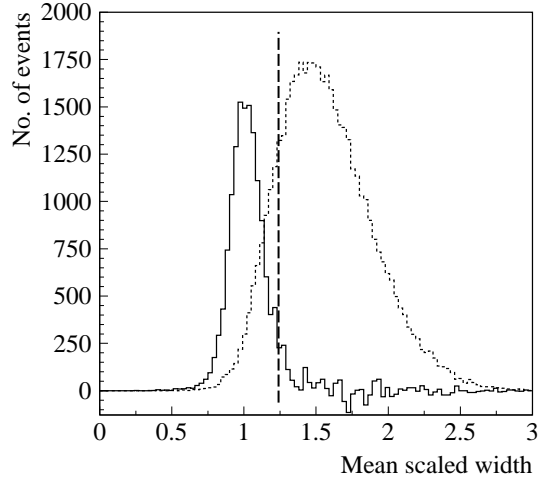


Fig. 2. Distribution in the *mean scaled width* for γ -ray showers (full line) after statistical subtraction of cosmic rays based on the off-source region, and for cosmic rays (dashed). The dashed line indicates the cut used to select γ -ray candidates.

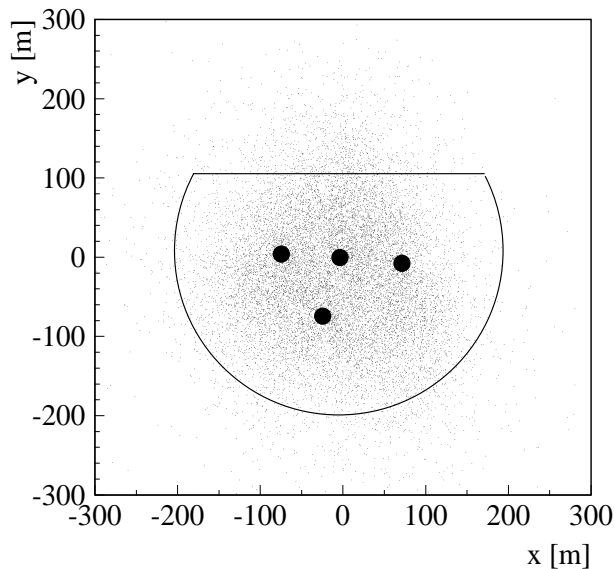


Fig. 3. Distribution of the core locations of events, after the cuts to enhance the fraction of γ -rays. Also indicated are the selection region and the telescope locations.

4 The shape of the Cherenkov light pool for γ -ray events

Using the technique described in the introduction, the intensity distribution in the Cherenkov light pool can now simply be traced by selecting events with the shower core at given distance r_i from a ‘reference’ telescope i and with a fixed image *size* a_i , and plotting the mean amplitude a_j of telescope j as a function of r_j . However, in this simplest form, the procedure is not very practical, given the small sample of events remaining after such additional cuts. To be able to use a larger sample of events, one has to

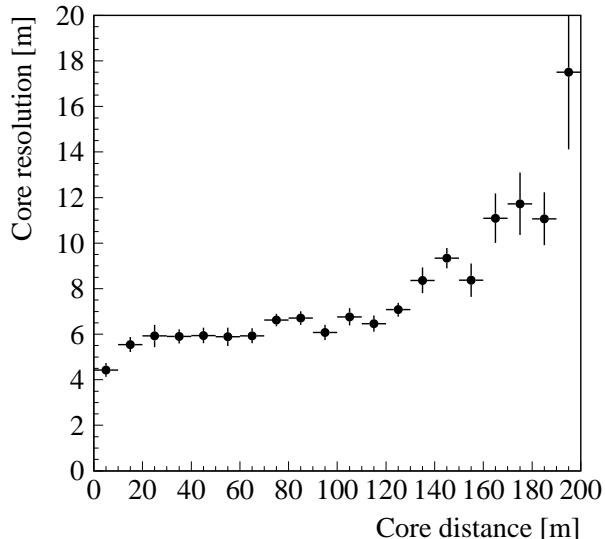


Fig. 4. Resolution in the core position as a function of the distance between the shower core and the central telescope, as determined from Monte Carlo simulations of γ -ray showers with energies between 1 and 2 TeV. The resolution is defined by fitting a Gaussian to the distribution of differences between the true and reconstructed coordinates of the shower impact point, projected onto the x and y axes of the coordinate system. Due to slight non-Gaussian tails, the rms widths of the distributions are about 20% larger.

- select events with a_i in a certain range, $a_{min} < a_i < a_{max}$, and plot a_j/a_i vs r_j , assuming that the shape of the light pool does not change rapidly with energy, and that one can average over a certain energy range
- repeat the measurement of $a_j(r_j)/a_i$ for different (small) bins in r_i , and combine these measurements after normalizing the distributions at some fixed distance
- Combine the results obtained for different pairs of telescopes i, j .

Care has to be taken not to introduce a bias due to the trigger condition. For example, one has to ensure that the selection criterion of at least three triggered telescopes is fulfilled regardless of whether telescope j has triggered or not, otherwise the selection might enforce a minimum image *size* in telescope j .

To avoid truncation of images by the border of the camera, only images with a maximum distance of 1.5° between the image centroid and the camera center were included, leaving a 0.6° margin to the edge of the field of view. Since the image of the source is offset by 0.5° from the camera center, a maximum

distance of 2.0° is possible between the source image and the centroid of the shower image.

Even after these selections, the comparison between data and shower models is not completely straight forward. One should not, e.g., simply compare data to the predicted photon flux at ground level since

- as is well known, the radial dependence of the density of Cherenkov light depends on the solid angle over which the light is collected, i.e., on the field of view of the camera
- the experimental resolution in the reconstruction of the shower core position causes a certain smearing, which is visible in particular near the break in the light distribution at the Cherenkov radius
- the selection of image pixels using the tail cuts results in a certain loss of photons; this loss is the more significant the lower the intensity in the image is, and the more diffuse the image is.

While the distortion in the measured radial distribution of Cherenkov light due to the latter two effects is relatively modest (see Fig. 5), a detailed comparison with Monte Carlo should take these effects into account by processing Monte-Carlo generated events using the same procedure as real data, i.e., by plotting the distance to the reconstructed core position rather than the true core position, and by applying the same tail cuts etc.

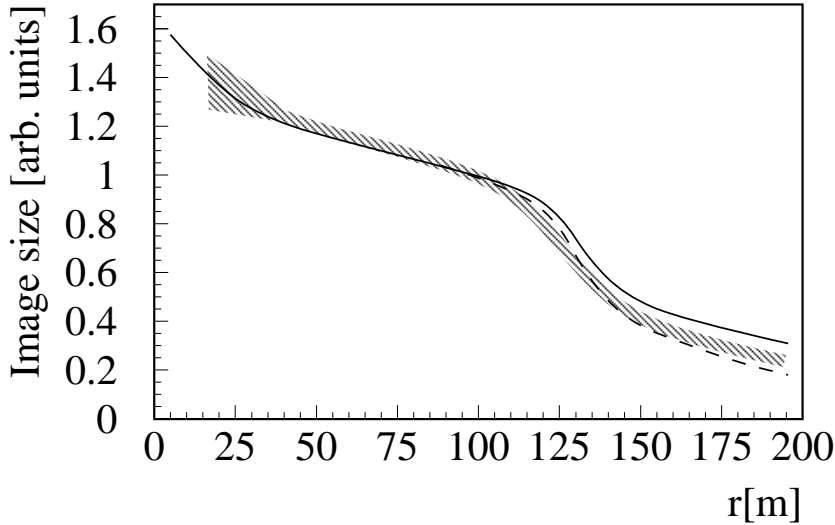


Fig. 5. Radial distribution of Cherenkov light for TeV γ -ray showers, for unrestricted aperture of the photon detector (full line), for a 2° aperture (dashed), and including the full camera simulation and image processing (shaded). The curves are normalized at $r \approx 100$ m.

For a first comparison between data and simulation, showers from the zenith (zenith angle between 10° and 15°) were selected. The range of distances r_i

from the shower core to the reference telescope was restricted to the plateau region between 50 m and 120 m. Smaller distances were not used because of the large fluctuations of image *size* close to the shower core, and larger distances were excluded because of the relatively steep variation of light yield with distance. The showers were further selected on an amplitude in the ‘reference’ telescope i between 100 and 200 photoelectrons, corresponding to a mean energy of about 1.3 TeV. Contamination of the Mrk 501 on-source data sample by cosmic rays was subtracted using an off-source region displaced from the optical axis by the same amount as the source, but in the opposite direction. The measured radial distribution (Fig. 6(a)) shows the expected features: a relatively flat plateau out to distances of 120 m, and a rapid decrease in light yield for larger distances.

The errors given in the Figure are purely statistical. To estimate the influence of systematic errors, one can look at the consistency of the data for different ranges in distance r_i to the ‘reference’ telescope, one can compare results for different telescope combinations, and one can study the dependence on the cuts applied. Usually, the different data sets were consistent to better than ± 0.05 units; systematic effects certainly do not exceed a level of ± 0.1 units. Within these errors, the measured distribution is reasonably well reproduced by the Monte-Carlo simulations.

Shower models predict that the distribution of light intensity varies (slowly) with the shower energy and with the zenith angle. Fig. 6 compares the distributions obtained for different *size* ranges a_i of 100 to 200, 200 to 400, and 400 to 800 photoelectrons at distances between 50 m and 120 m, corresponding to mean shower energies of about 1.3, 2.5, and 4.5 TeV, respectively. We note that the intensity close to the shower core increases with increasing energy. This component of the Cherenkov light is generated by penetrating particles near the shower core. Their number grows rapidly with increasing shower energy, and correspondingly decreasing height of the shower maximum. The increase in the mean light intensity at small distances from the shower core is primarily caused by long tails distribution of image *sizes* towards large *size*; the median *size* is more or less constant. The observed trends are well reproduced by the Monte-Carlo simulations.

The dependence on zenith angle is illustrated in Fig. 7, where zenith angles between 10° and 15° , 15° and 25° , 25° and 35° , and 35° and 45° are compared. Events were again selected for an image *size* in the ‘reference’ telescope between 100 and 200 photoelectrons, in a distance range of 50 m to 120 m ¹. The corresponding mean shower energies for the four ranges in zenith angle are about 1.3 TeV, 1.5 TeV, 2 TeV, and 3 TeV. For increasing zenith angles, the distribution of Cherenkov light flattens for small radii, and the diameter of the

¹ Core distance is always measured in the plane perpendicular to the shower axis

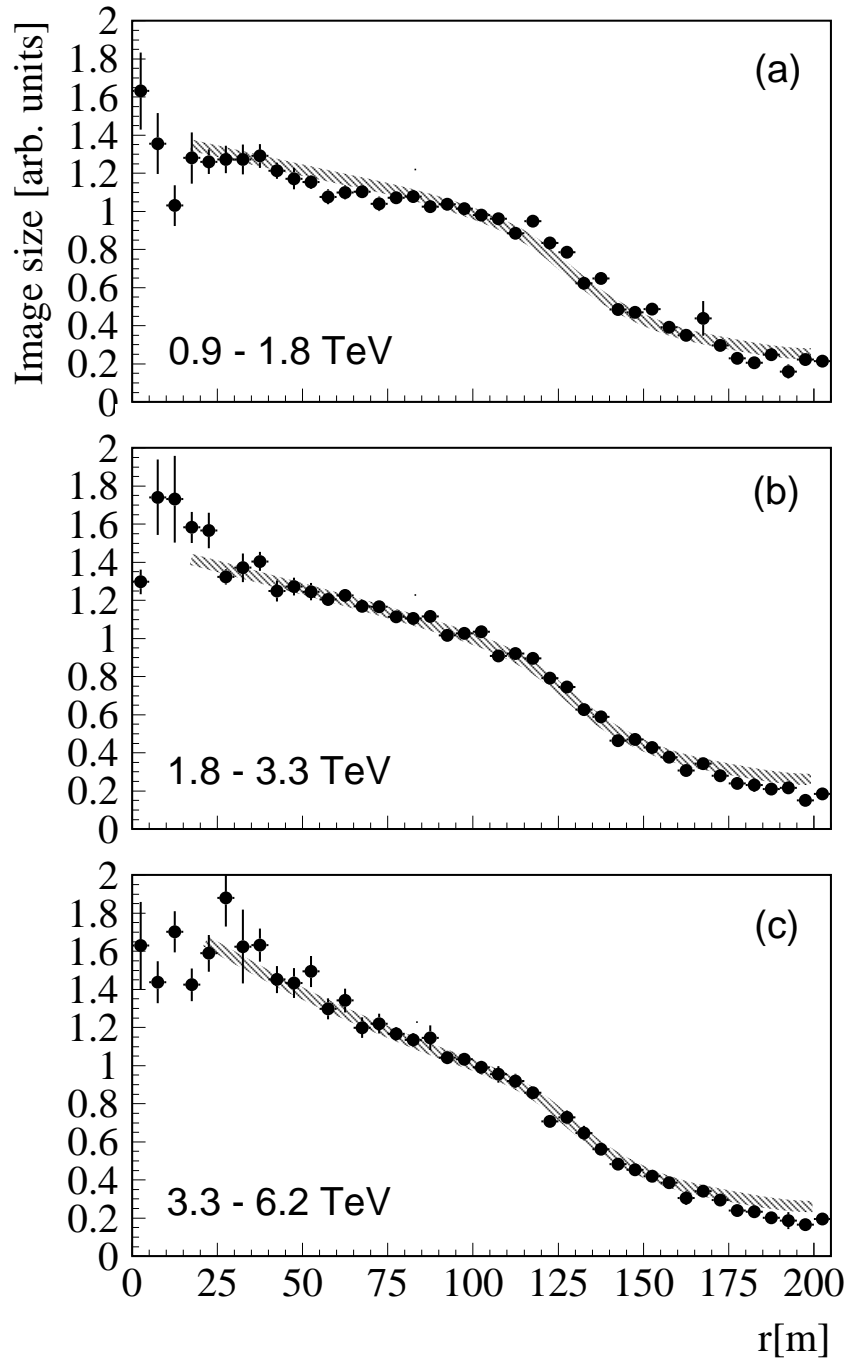


Fig. 6. Light yield as a function of shower energy, for image *size* in the reference telescope between 100 and 200 photoelectrons (a), 200 and 400 photoelectrons (b), and 400 to 800 photoelectrons (c). Events were selected with a distance range between 50 m and 120 m from the reference telescope, for zenith angles between 10° and 15° . The shaded bands indicate the Monte-Carlo results. The distributions are normalized at $r \approx 100$ m. Only statistical errors are shown.

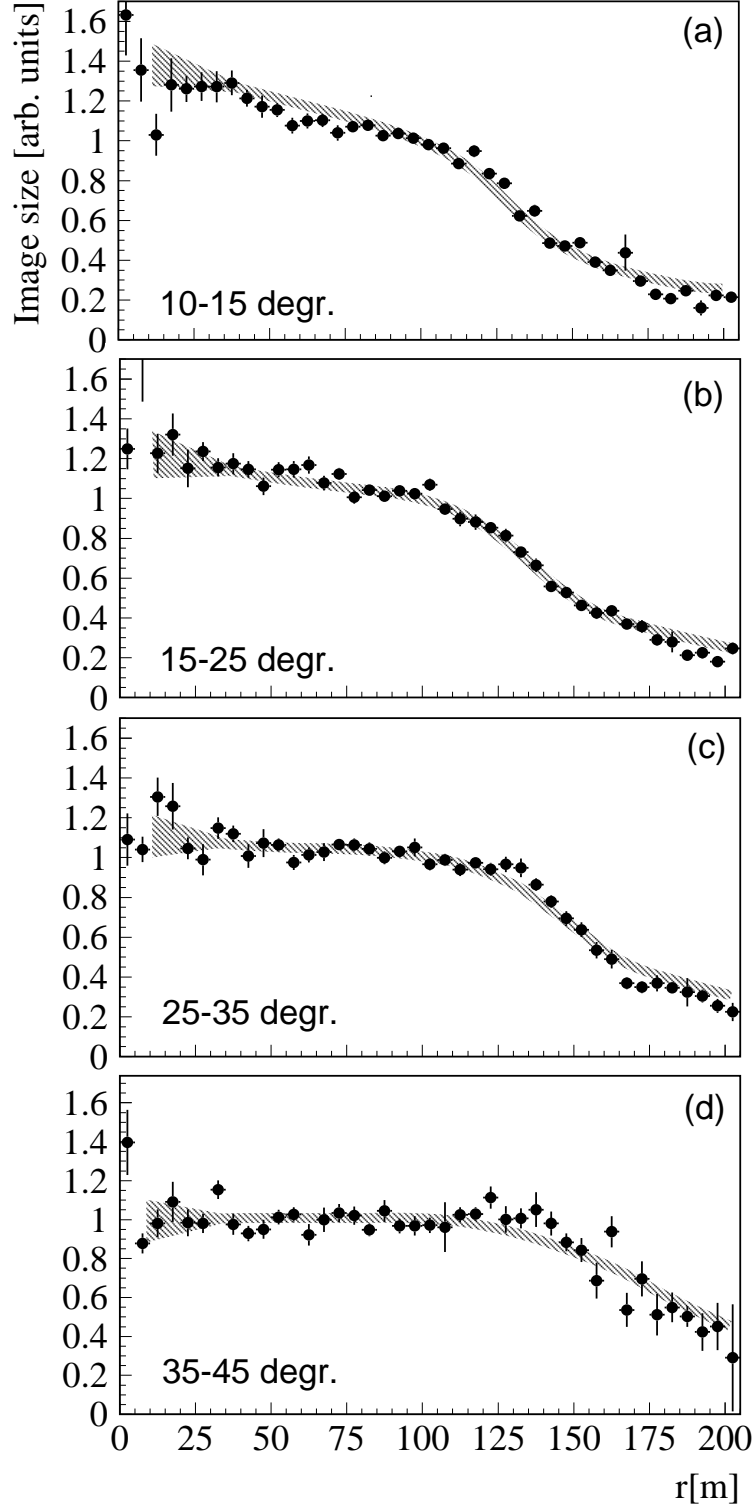


Fig. 7. Light yield as a function of core distance, for zenith angles between 10° and 15° (a), 15° and 25° (b), 25° and 35° (c), and 35° and 45° (d). Events were selected with a distance range between 50 m and 120 m from the reference telescope, and an image *size* between 100 and 200 photoelectrons in the reference telescope. The shaded bands indicate the Monte-Carlo results. The distributions are normalized at $r \approx 100$ m. Only statistical errors are shown.

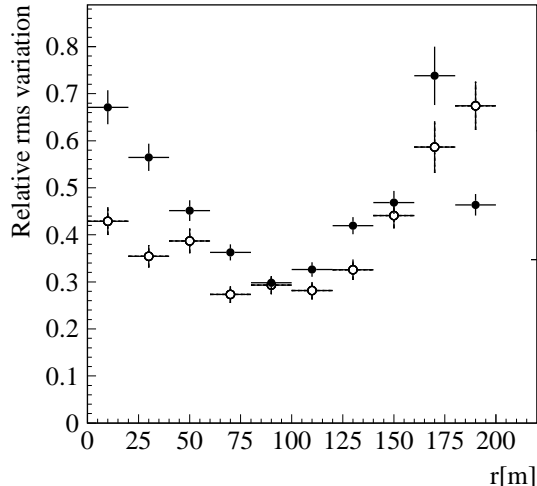


Fig. 8. Relative variation in the *size* ratio a_j/a_i as a function of r_j , for r_i in the range 50 m to 120 m, and for image *size* in the ‘reference’ telescope between 100 and 200 photoelectrons. Full circles refer to zenith angles between 10° and 15° , open circles to zenith angles between 25° and 35° .

light pool increases. Both effects are expected, since for larger zenith angles the distance between the telescope and the shower maximum grows, reducing the number of penetrating particles, and resulting in a larger Cherenkov radius. The simulations properly account for this behaviour.

It is also of some interest to consider the fluctuations of image *size*, $\Delta(a_j/a_i)$. Fig. 8 shows the relative rms fluctuation in the *size* ratio, as a function of r_j , for small (10° to 15°) and for larger (25° and 35°) zenith angles. The fluctuations are minimal near the Cherenkov radius; they increase for larger distances, primarily due to the smaller light yield and hence larger relative fluctuations in the number of photoelectrons. In particular for the small zenith angles, the fluctuations also increase for small radii, reflecting the large fluctuations associated with the penetrating tail of the air showers. For larger zenith angles, this effect is much reduced, since now all shower particles are absorbed well above the telescopes; more detailed studies show that already zenith angles of 20° make a significant difference.

5 Summary

The stereoscopic observation of γ -ray induced air showers with the HEGRA Cherenkov telescopes allowed for the first time the measurement of the light distribution in the Cherenkov light pool at TeV energies, providing a consistency check of one of the key inputs for the calculation of shower energies based on the intensity of the Cherenkov images. The light distribution shows a characteristic variation with shower energy and with zenith angle. Data are

well reproduced by the Monte-Carlo simulations.

Acknowledgements

The support of the German Ministry for Research and Technology BMBF and of the Spanish Research Council CYCIT is gratefully acknowledged. We thank the Instituto de Astrofísica de Canarias for the use of the site and for providing excellent working conditions. We gratefully acknowledge the technical support staff of Heidelberg, Kiel, Munich, and Yerevan.

References

- [1] T.C. Weekes, *Space Science Rev.* 75 (1996) 1; M. F. Cawley and T.C. Weekes, *Experimental Astronomy* 6 (1996) 7.
- [2] A. Daum et al., *Astroparticle Phys.* 8 (1997) 1.
- [3] W. Hofmann, *Proceedings of the Int. Workshop "Towards a Major Atmospheric Cherenkov Detector V"*, Kruger Park, (1997), in press, and *astro-ph/9710297*.
- [4] *Handbook of Geophysics and Space Environments*, S.L. Valley (Ed.), McGraw-Hill.
- [5] F.X. Kneizys et al., "The MODTRAN 2/3 Report and LOWTRAN 7 Model" (L.W. Abreu and G.P. Anderson, Eds.), Philips Laboratory, Hanscom Air Force Base, MA 01731-3010 (1996).
- [6] A. Konopelko, *Proceedings of the Int. Workshop "Towards a Major Atmospheric Cherenkov Detector V"*, Kruger Park, (1997), in press.
- [7] F.A. Aharonian et al., *Astroparticle Phys.* 6 (1997) 343.
- [8] F.A. Aharonian et al., *Astron. Astropys.* 327 (1997) L5.
- [9] G. Hermann, *Proceedings of the Int. Workshop "Towards a Major Atmospheric Cherenkov Detector IV"*, Padua, (1995), M. Cresti (Ed.), p. 396.
- [10] N. Bulian et al., *Astroparticle Phys.* 8 (1998) 223.
- [11] G. Pühlhofer et al., *Astroparticle Phys.* 8 (1997) 101.
- [12] M. Heß, Ph.D. Thesis, Heidelberg 1998.
- [13] A.M. Hillas, *Proc. 19th ICRC (La Jolla, 1985) Vol. 3*, 445.
- [14] A. Kohnle et al., *Astroparticle Phys.* 5 (1996) 119.

- [15] J. Quinn et al., *Astrophys. J.* 456 (1996) L83.
- [16] S.M. Bradbury et al., *Astron. Astrophys.* 320 (1997) L5.
- [17] R.J. Protheroe et al., *Proc. of the 25 Int. Cosmic Ray Conf., Durban, 1997,* and astro-ph 9710118.
- [18] A.K. Konopelko et al., *Astroparticles Physics* 4 (1996) 199.
- [19] D. Heck et al., *Technical Report FZKA 6019, Forschungszentrum Karlsruhe,* 1998.
- [20] M. Hemberger, *Ph.D. Thesis, Heidelberg* 1998.
- [21] K. Bernlöhr, *in preparation.*